

Adaptive wettability-enhanced surfaces ordered on molded etched substrates using shrink film

This article has been downloaded from IOPscience. Please scroll down to see the full text article.

2013 Smart Mater. Struct. 22 014014

(<http://iopscience.iop.org/0964-1726/22/1/014014>)

View [the table of contents for this issue](#), or go to the [journal homepage](#) for more

Download details:

IP Address: 169.234.24.47

The article was downloaded on 15/01/2013 at 19:58

Please note that [terms and conditions apply](#).

Adaptive wettability-enhanced surfaces ordered on molded etched substrates using shrink film

Shreshta Jayadev¹, Jonathan Pegan¹, David Dyer, Jolie McLane, Jessica Lim and Michelle Khine

Department of Biomedical Engineering, University of California, Irvine, Irvine, CA 92697, USA

E-mail: mkhine@uci.edu

Received 24 July 2012, in final form 15 November 2012

Published 18 December 2012

Online at stacks.iop.org/SMS/22/014014

Abstract

Superhydrophobic surfaces in nature exhibit desirable properties including self-cleaning, bacterial resistance, and flight efficiency. However, creating such intricate multi-scale features with conventional fabrication approaches is difficult, expensive, and not scalable. By patterning photoresist on pre-stressed shrink-wrap film, which contracts by 95% in surface area when heated, such features over large areas can be obtained easily. Photoresist serves as a dry etch mask to create complex and high-aspect ratio microstructures in the film. Using a double-shrink process, we introduce adaptive wettability-enhanced surfaces ordered on molded etched (AWESOME) substrates. We first create a mask out of the children's toy 'Shrinky-Dinks' by printing dots using a laserjet printer. Heating this thermoplastic sheet causes the printed dots to shrink to a fraction of their original size. We then lithographically transfer the inverse pattern onto photoresist-coated shrink-wrap polyolefin film. The film is then plasma etched. After shrinking, the film serves as a high-aspect ratio mold for polydimethylsiloxane, creating a superhydrophobic surface with water contact angles $>150^\circ$ and sliding angles $<10^\circ$. We pattern a microarray of 'sticky' spots with a dramatically different sliding angle compared to that of the superhydrophobic region, enabling microtiter-plate type assays without the need for a well plate.

 Online supplementary data available from stacks.iop.org/SMS/22/014014/mmedia

(Some figures may appear in colour only in the online journal)

1. Introduction

Superhydrophobic surfaces enable free movement of water across a surface due to water's high contact angle (CA) and low sliding angle (SA). In nature, this desirable property exhibited by lotus leaves [1], springtails (*Collembola*, *Entognatha*) [2], and termite wings (*Nasutitermes* sp.) [3] allows for remarkable characteristics including self-cleaning, bacterial resistance, and flight efficiency. This phenomenon can be explained by a model created by Cassie and Baxter [4] in which water can only contact the peaks of

a roughened surface due to the formation of air pockets between the water and the surface. This decreases the contact area. For multi-scale (nano to micro) roughness substrates such as the lotus leaf, this model predicts well the equilibrium state between the solid and liquid phases [5]. Such multi-scale superhydrophobic surfaces can be achieved artificially through either structural [6, 7] or chemical [8, 9] alterations. Current fabrication techniques employ complex production methods to create highly organized and intricate structures. Simplifying fabrication and enabling its structural integration into existing materials would enable it for a range of materials for various biomedical (e.g. implants, coatings) as well as consumer applications.

¹ Both authors contributed equally to this work.

While microstructures fabricated in pre-stressed thermoplastics have been demonstrated before, either by depositing materials on the plastic which retract and reflow with the plastic [10–13] or by etching directly into the plastic [14], patterning at high resolution via photolithography and then etching into the substrate has not heretofore been demonstrated. To make high-aspect ratio microstructures in the thermoplastic polystyrene (PS) sheet, pre-defined shadow masks (e.g. commercial transmission electron microscopy (TEM) grids or gold-coated home-made free-standing polymeric microstructures) are used with reactive ion etching (RIE) [14, 15]. However, with this approach, the features are pre-defined by the features of the shadow mask. In order to create custom micro-features of any design rapidly, as is critical for MEMS and microfluidic applications, the ability to combine with a custom mask is necessary. We introduce adaptive wettability-enabled surfaces ordered on molded etched (AWESOME) substrates in which we pattern a microarray of ‘sticky’ spots with dramatically different sliding angles compared to those of the surrounding superhydrophobic region.

Superhydrophobic patterns have applications in MEMS and microfluidics, with selectively patternable resistance patches for liquids [16–18]. It has also been shown that superhydrophobic surfaces can resist adhesion of cells and proteins [19]. Importantly, superhydrophobic polymer surfaces can have significant industrial and technological relevance in terms of anti-oxidation, biocompatibility, and contamination prevention [20]. The ability to wet the surface depends on the surface energies of the solid–gas interface. Water contact angle (CA) measurements are used to quantify this surface wetting property. CA for superhydrophilic surfaces varies between 0° and 30° while hydrophilic surfaces have values ranging from 30° to 90° . On the other hand, hydrophobic surfaces have $CA > 90^\circ$ and superhydrophobic surfaces have $CA > 150^\circ$. Another important parameter is the sliding angle (SA) of a water drop on the surface. SA is a representation of the adhesive forces between the liquid and the solid surface. The greater the adhesion, the higher the SA. Typically, for superhydrophobic surfaces $SA < 10^\circ$ have been reported [21, 22].

A variety of fabrication techniques have been reported to functionalize a surface to be superhydrophobic, which include alignment of densely packed PS nanotubes [23], plasma polymerization [24], and gel-like roughened polypropylene [25]. Another widely described technique for the creation of superhydrophobic surfaces is by fluorination [26, 27]. Fluorination causes a change in surface roughness and the fluorinated groups help to lower the surface energy; however, this process is expensive and, due to aging from change in environmental conditions like moisture and temperature, such surfaces tend to return to their original non-superhydrophobic state [28].

Photolithography is an integral and standard step in micro-manufacturing. Features can be created by selectively exposing certain areas of a thin photosensitive polymer layer coated onto glass or silicon. The cross-linked photoresist features defined in this step can then be used as an

etch mask to transfer the pattern into the substrate below. In fact, plasma etching of photolithographically defined regions is the main approach for micropatterning [29]. However, conventional wisdom suggests that standard photolithography is not compatible with polymer substrates, as polymers tend to react with organic solvents and developers and typically cannot withstand temperatures $> 140^\circ\text{C}$ [30]. Yet, the many benefits of plastic substrates for electronics and microelectromechanical systems (MEMS) applications, including durability, flexibility, transparency, and portability, have incited the development of more elaborate fabrication processes such as hot-embossing and nano-imprint lithography (NIL) to circumvent this limitation [31, 32].

If superhydrophobic surfaces could be made inexpensive, robust, and patternable, simpler point of care (POC) diagnostic devices could be realized. Currently, molecular assays are typically performed in microtiter plates such as 384 well plates. However, in addition to their expense, such well plates necessitate larger working volumes (20–120 μl) and have inherently significantly more interfacial contact area with the substrate [33]. The push to make smaller wells drives up costs and, more detrimentally, the ratio of contact area to volume.

To this end, there has been much work with alternative options for low cost POC diagnostics such as paper-based microfluidics or microfluidic paper analytical devices (μPADs) [34]. However, μPADs rely on absorption of the fluidics into the porous paper. Therefore, such an approach is inherently limited in its sensitivity as well as its inability to remove the solution for subsequent analyses [34]. While this strategy of tuning surface wettability for droplet manipulation has been demonstrated, it has been heretofore limited in the spot size to the mm scale, resulting in rather large working volumes of solution [33]. In contrast, because we can achieve a $>20\times$ size reduction after patterning due to our shrinking process, we can easily achieve spot sizes down to the micron scale.

In order to create AWESOME substrates, we employed a simple double-shrink process. First a mask was created from PS sheets by simply printing dots using a commercial laserjet printer. Upon retraction of the thermoplastic sheet, the printed dots shrunk to a fraction of their original size. These patterns were then lithographically transferred onto polyolefin (PO) shrink-wrap film coated with negative photoresist. Importantly, we demonstrated that the patterned photoresist was an effective mask for the oxygen plasma used to etch into the PO, and regions beneath the photoresist were protected and therefore unaffected by the oxygen plasma etch. After the features were etched into PO, the photoresist was removed and then the substrate was shrunk, carrying the photoresist-defined features with it, as illustrated in figure 1, for a total reduction in size of almost 99% in surface area from the printed PS mask to the shrunk PO substrate. This etched PO was then molded to create high-aspect ratio micropillars with nanostructuring in polydimethylsiloxane (PDMS). Because of the nanostructuring on micro-features, we effectively achieved superhydrophobic surfaces in PDMS without any chemical modifications [16, 22].

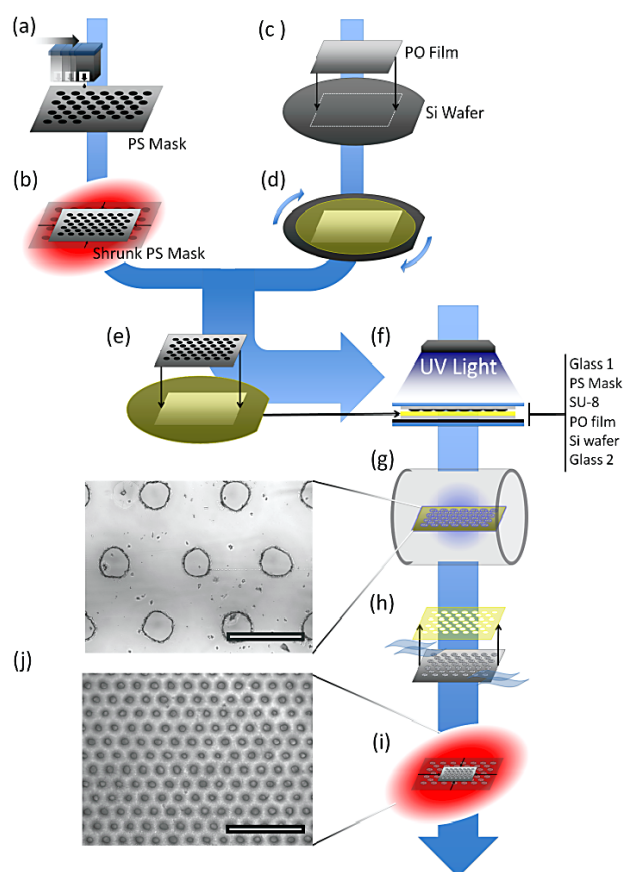


Figure 1. PO mold fabrication process. The PS sheet was printed with a laserjet printer. (a) The PS sheet was heated using a heat gun to shrink it 65% by area. (b) PO film was placed on Si wafer and taped down. (c) SU-8 5 photoresist was then spun at 1000 rpm onto PO. (d) Shrunken PS was used as a mask by placing it top-down on top of the SU-8 layer. (e) Mask and wafer were sandwiched using glass and exposed to UV light. (f) PO film was developed and later etched in O_2 plasma. (g) The SU-8 5 layer was stripped away. (h) PO film was then heated with a heat gun to shrink it 95% by area. (i) Feature sizes were miniaturized by 99% from the original CAD drawing. Bright field image of the PO mold: (j) pre-shrunk (top) and shrunk (bottom). The scale bar is $250 \mu\text{l}$.

Therefore, we have developed a microfabrication approach to rapidly create customizable substrates by integrating photolithography and plasma etching with PO film processing. Notably, we moved away from more aggressive RIE and used only an inexpensive benchtop plasma etcher common to most materials laboratories.

Importantly, this approach enabled us to pattern a microarray of ‘sticky’ spots on the superhydrophobic sheet, resulting in dramatically different SA than the superhydrophobic regions of the sheet [35]. ‘Sticky’ spots are flat, unstructured areas of non-superhydrophobicity on the surface that the droplets will preferentially stick to and not easily roll-off of, unlike the rest of the surface. Because the SA of the superhydrophobic areas is so low, if a droplet is introduced to the surface, it will roll to and anchor on the non-superhydrophobic sticky spot only.

To create these sticky spots, we selectively protect areas from plasma etching by creating an array of spots protected

by photoresist. The spots are printed on the PS mask and the design is further translated into the photoresist, which protects the PO surface during etching. When molded with PDMS, these regions are essentially flat PDMS with high SA. These spots enabled us to develop microtiter-plate type assays of arbitrary size without the need for a well plate as commonly used in PDMS. The droplets placed on these ‘sticky’ regions were easily manipulated and mixed. They could also be transported on these regions without smearing or release.

2. Materials and methods

2.1. PS mask fabrication

The mask used for photolithography was fabricated by printing black toner onto PS sheet using a commercial laserjet printer (HP Color LaserJet CP2025, USA). This plastic sheet was then heated above the glass transition temperature (T_g) of 100°C to rapidly shrink ($<15 \text{ s}$) it by 65% in area using a heat gun (Steinel® professional heat gun 1810 S, MN). The printed features shrink along with the plastic sheet.

2.2. PO film photolithography

A $3 \text{ in} \times 3 \text{ in}$ piece of PO film (Sealed Air, 1 mil on 3 mil polyester backing, 955D) was taped onto a 4 in wafer using tape (Scotch®). OmniCoat™ (MicroChem®, MA) was spun onto the wafer with taped PO at 3000 rpm for 30 s and baked for 6 min 30 s at 95°C on a hot plate. SU-8 5 (MicroChem®), a negative photoresist, was spun onto this wafer at 1000 rpm for 30 s to obtain $15 \mu\text{m}$ thickness and soft baked at 65°C for 2 min and 95°C for 5 min. After the wafer was allowed to cool, SU-8 5 was exposed under a UV lamp at 500 W for 9 s using the mask created earlier. Post-exposure bake was performed at 65°C for 1 min and 95°C for 2 min and developed in SU-8 Developer (MicroChem®) for 3 min and rinsed. An array of circular features was left uncovered by the SU-8.

2.3. PO film etching, shrinking, and soft lithography

The patterned PO was etched in oxygen plasma (SPI Plasma Prep II™) for 15 min at 150 mTorr μm vacuum chamber pressure and 10 psi oxygen pressure at 90 mA. During the plasma treatment, The SU-8 layer protects the PO surface from being etched except for the uncovered areas causing wells to be carved into the PO. SU-8 was then stripped away in a bath of Nano™ Remover PG (MicroChem®) for 1 h at 70°C . The PO sample was then rinsed in DI water, dried, and shrunk under a heat gun, at temperatures above the 125°C T_g for PO, forming an array of microwells. A PDMS (Sylgard® 184, Dow Corning Corporation) mold of micropillars was made from the shrunk PO microwells array. The resulting PDMS molded micropillar surfaces were used for characterizing the hydrophobicity of the surface.

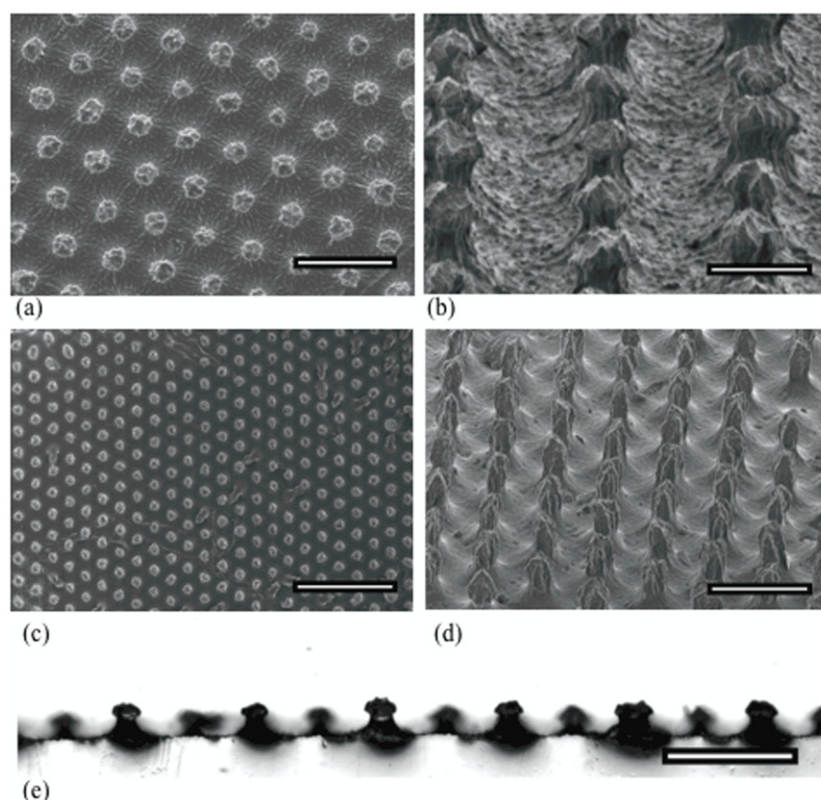


Figure 2. SEM images of PDMS molded from a microwell array. A top-down view of the PDMS surface molded from a microwell array fabricated using a Shrinky-Dinks mask (a) and using Mylar mask (c). The scale bar is $100\ \mu\text{m}$. The inclined image of micropillars on PDMS molded from the Shrinky-Dinks mask patterned microwell array (b) and the Mylar mask (d). The scale bar is $30\ \mu\text{m}$. (e) The cross section of PDMS molded from the Shrinky-Dinks mask patterned array. The scale bar is $100\ \mu\text{m}$.

2.4. Superhydrophobicity characterization

CA experiments were conducted by dropping a $5\ \mu\text{l}$ water droplet onto the PDMS surface using a micropipette. Using a digital single lens reflex (DSLR) camera and backlighting, close-up images were taken to see the contact point of the water droplet with the surface. Measurements of the CA were obtained using an ImageJ [36] based plug-in, low bond axisymmetric drop shape analysis (LB-ADSA), which was based on a perturbation solution of the axisymmetric Laplace equation [37]. This experiment was repeated for several droplets on four separate PDMS molds ($n = 20$) obtained from separately fabricated microwell arrays. In order to measure the SA, the PDMS molds were placed on a flat glass slide attached to a rotating stage and $10\ \mu\text{l}$ of water was placed onto the surface. The movement was recorded ($n = 15$) while manually rotating the stage gradually until the droplet rolled-off. We defined the angle at which the drop was displaced from its initial position as the SA.

3. Results and discussion

Wells of $23.2\ \mu\text{m}$ (± 2.4) in diameter and $28.7\ \mu\text{m}$ (± 2.1) in depth were achieved after 15 min of oxygen plasma etching and shrinking of the PO film. Before shrinking, the wells were $101.4\ \mu\text{m}$ (± 4.8) in diameter and $2.1\ \mu\text{m}$ (± 0.7) in depth. Figure 2(a) shows the top-down view of the scanning

electron microscope (SEM, Hitachi S-4700-2FESEM) image of PDMS molded from a microwell array fabricated using the PS mask. An image of 60° inclination of the same mold is seen in figure 2(b). The cross section of the PDMS mold in figure 2(e) presents interesting surface modification with mushroom-like structures having roughened surface on the tip of each of the pillars.

Next, we characterized the superhydrophobicity of the surface by performing water contact angle measurements. PDMS was chosen as a molding material for its excellent fidelity, biocompatibility, and because it is inherently more hydrophobic than flat PO (CA of 89.5° , $\pm 1.1^\circ$). Several droplets on three separate PDMS molds ($n = 20$) were obtained from separately fabricated microwell arrays. Figure 3 quantifies the difference in contact angle between untreated PDMS CA = 109.6° (± 4.9), PDMS molded from plasma treated PO CA = 147.6° (± 4.4), and PDMS molded from PS mask patterned PO CA = 157.4° (± 3.6). The average SA for this surface was recorded to be 6.9° (± 0.7).

Further, to evaluate the possibility of increasing superhydrophobicity by decreasing feature size, we used a Mylar mask (FineLine Imaging) in place of the PS mask used previously to pattern $50\ \mu\text{m}$ dots onto PO and repeated the aforementioned process to obtain PDMS mold with pillars of size $8.1\ \mu\text{m}$ (± 0.7) in diameter and $15.5\ \mu\text{m}$ (± 0.9) in height, as seen in the SEM images of figures 2(c) and (d). Water contact angle measurements were repeated

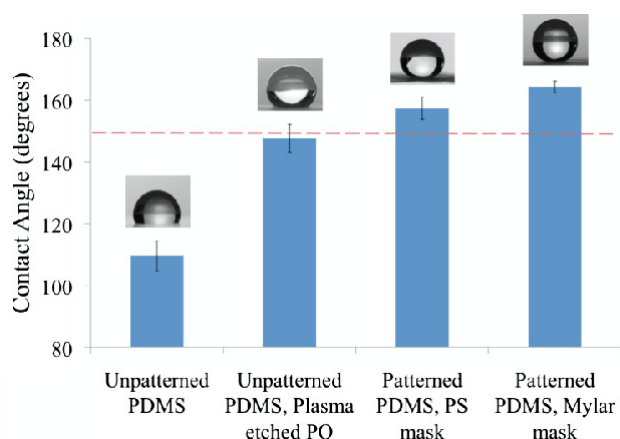


Figure 3. The differences in CA between untreated PDMS, PDMS from plasma treated PO, PDMS from PS mask patterned PO, and PDMS from Mylar mask patterned PO.

on three separate PDMS molds with five droplets on each ($n = 15$). This experiment revealed an increase in CA of 7° from the initial CA of $157.4^\circ (\pm 3.6)$ to a higher CA of $164.3^\circ (\pm 1.9)$ (figure 3) and a lower SA of $5.8^\circ (\pm 0.3)$. Notably, these micropillars do not buckle under the weight of the water droplets at the low volumes used in this study. De Angelis *et al* has shown similar results with comparable pillar structures [38].

Finally, to demonstrate the ability to rapidly and easily pattern various designs, we create AWESOME substrates in which we patterned a microarray of ‘sticky’ spots with a dramatically different sliding angle compared to those of the surrounding superhydrophobic region. We propose that this could be an inexpensive alternative substrate for molecular assays. Figures 4(a)–(c) shows $2 \mu\text{l}$ droplets of water on the patterned circular bald spots (flat PDMS) on the otherwise superhydrophobic surface at 0° , 90° , and 180° demonstrating that we can transport these assays without fear of mixing or

smearing. Mixing can also be easily achieved without fear of losing solution at the non-detection spots due to the extreme hydrophobicity figures 4(d)–(f).

4. Conclusion

We have demonstrated a simple process to create AWESOME surfaces on PDMS without the need for any type of chemical surface modification. Therefore, the surface is robust and there is no risk of the surface delaminating or chemicals leaching. Using shrunk PS sheets as a mask for photolithography, we pattern onto PO shrink film. Further, using a benchtop plasma etcher, features are directly etched into the uncovered areas of the PO film, creating high-aspect ratio wells in the PO film. A total reduction of almost 99% from original patterned area is obtained after shrinking the etched film. The surface of the PDMS molded from this is superhydrophobic in nature due to the presence of hierarchical nano- and micro-scale pillars. Importantly, the PO mold can be remolded numerous times while maintaining the superhydrophobic features. Characterizing this surface provided us with CA = $157.4^\circ (\pm 3.6)$ and an SA of $6.9^\circ (\pm 0.7)$. To demonstrate the functionality of this approach we patterned ‘sticky’ spots composed of non-etched, flat PDMS, which showed easy manipulation and mixing of water droplets with an order of magnitude lower volumes ($2 \mu\text{l}$) than that achievable with 384 microtiter plates. This lends itself to the potential for low cost POC diagnostic devices with higher possible sensitivity than paper-based microfluidics. Moreover, because all this is performed in the commonly used PDMS, this approach is easily adoptable and integrated into microfluidic processing. The ability to pattern using photoresist on shrinkable films allows us to create adaptive superhydrophobic surfaces with arbitrary patterns, enabling new low cost substrates for molecular assays.

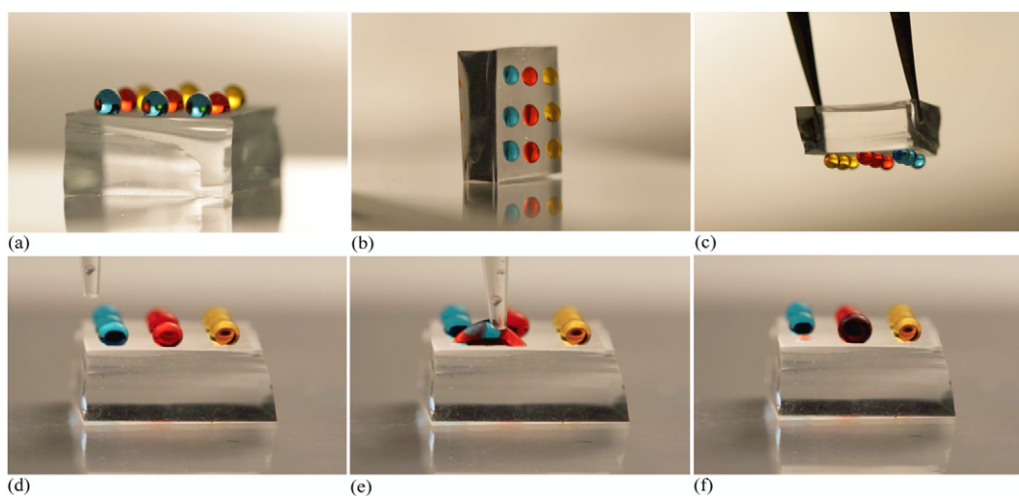


Figure 4. Droplets of colored food dye on AWESOME substrate at 0° , 90° , and 180° ((a)–(c)) demonstrating the ability to move the substrate without disturbing the spots. A sequence of images showing mixing of superhydrophobic droplets. A movie of this can be found in the supplementary information (available at stacks.iop.org/SMS/22/014014/mmedia).

Acknowledgment

This work was supported in part by the National Institutes of Health through the NIH Director's New Innovator Award Program Grant No. 1DP2OD007283.

References

- [1] Cheng Y T, Rodak D E, Wong C A and Hayden C A 2006 *Nanotechnology* **17** 1359–62
- [2] Helbig R, Nickerl J, Neinhuis C and Werner C 2011 *PLoS One* **6** 9
- [3] Watson G S, Cribb B W and Watson J A 2011 *PLoS One* **6** e24368
- [4] Cassie A B D and Baxter S 1944 *Faraday Soc.* **40** 546–51
- [5] Cheng Y T, Rodak D E, Wong C A and Hayden C A 2006 *Nanotechnology* **17** 1359–62
- [6] Xu Q F, Wang J N and Sanderson K D 2010 *ACS Nano* **4** 2201–9
- [7] Ebril H Y, Demirel A L, Avci Y and Mert O 2003 *Science* **299** 1377–80
- [8] Gomez G B, Flendrig L M and Cooper J M 2010 *Langmuir* **26** 7248–53
- [9] Öner D and McCarthy T J 2000 *Langmuir* **16** 3453–6
- [10] Liu X, Chakraborty A and Luo C 2010 *J. Micromech. Microeng.* **20** 095025
- [11] Nguyen D, Sa S, Pegan J D, Rich B, Xiang G, McCloskey K E, Manilay J O and Khine M 2009 *Lab Chip* **9** 3338–44
- [12] Lee M H, Huntington M D, Zhou W, Yang J-C and Odom T W 2010 *Nano Lett.* **11** 311–5
- [13] Dyer D, Shreim S, Jayadev S, Lew V, Botvinick E and Khine M 2011 *Appl. Phys. Lett.* **99** 034102
- [14] Zhao X-M, Xia Y, Schueller O J A, Qin D and Whitesides G M 1998 *Sensors Actuators A* **65** 209–17
- [15] Zhao X-M, Xia Y, Qin D and Whitesides G M 1997 *Adv. Mater.* **9** 251–4
- [16] Cortese B, D'Amone S, Manca M, Viola I, Cingolani R and Gigli G 2008 *Langmuir* **24** 2712–8
- [17] Oliveira N M, Neto A I, Song W and Mano J F 2010 *Appl. Phys. Express* **3** 085205 085201 to 085205–085203
- [18] Zhai L, Berg M C, Cebeci F Ç, Kim Y, Milwid J M, Rubner M F and Cohen R E 2006 *Nano Lett.* **6** 1213–7
- [19] Fan H et al 2009 *Small* **5** 2144–8
- [20] Shang H M, Wang Y, Takahashi K, Cao G Z, Li D and Xia Y N 2005 *J. Mater. Sci.* **40** 3587–91
- [21] Tserepi A D, Vlachopoulou M-E and Gogolides E 2006 *Nanotechnology* **17** 3977
- [22] Jin M, Feng X, Xi J, Zhai J, Cho K, Feng L and Jiang L 2005 *Macromol. Rapid Commun.* **26** 1805–9
- [23] Jin M, Feng X, Feng L, Sun T, Zhai J, Li T and Jiang L 2005 *Adv. Mater.* **17** 1977–81
- [24] Teare D O H, Spanos C G, Ridley P, Kinmond E J, Roucoules V, Badyal J P S, Brewer S A, Coulson S and Willis C 2002 *Chem. Mater.* **14** 4566–71
- [25] Taurino R, Fabbri E, Messori M, Pilati F, Pospiech D and Synytska A 2008 *J. Colloid Interface Sci.* **325** 149–56
- [26] Woodward I, Schofield W C E, Roucoules V and Badyal J P S 2003 *Langmuir* **19** 3432–8
- [27] Cho W K, Kang S M, Kim D J, Yang S H and Choi I S 2006 *Langmuir* **22** 11208–13
- [28] Chan C M, Ko T M and Hiraoka H 1996 *Surf. Sci. Rep.* **24** 1–54
- [29] Gogolides E, Constantoudis V, Kokkoris G, Kontziampasis D, Tsougeni K, Boulousis G, Vlachopoulou M and Tserepi A 2011 *J. Phys. D: Appl. Phys.* **44** 174021
- [30] Lee H, Hong S, Yang K and Choi K 2006 *Microelectron. Eng.* **83** 323–7
- [31] Bubendorfer A, Liu X and Ellis A V 2007 *Smart Mater. Struct.* **16** 367–71
- [32] Lee H, Hong S, Yang K and Choi K 2006 *Appl. Phys. Lett.* **88** 143112
- [33] Balu B, Berry A D, Hess D W and Breedveld V 2009 *Lab Chip* **9** 3066–75
- [34] Martinez A W, Phillips S T and Whitesides G M 2008 *Proc. Natl Acad. Sci. USA* **105** 19606–11
- [35] Guo S S, Sun M H, Shi J, Huang Y J, Huang W H, Combellas C and Chen Y 2007 *Microelectron. Eng.* **84** 1673–6
- [36] Abramoff M D, Magalhaes P J and Ram S J 2004 *Biophotonics* **11** 36–42
- [37] Stalder A F, Melchior T, Müller M, Sage D, Blu T and Unser M 2010 *Colloids Surf. A* **364** 72–81
- [38] De Angelis F, Gentile F, Mecarini F, Das G and Moretti M 2011 *Nature Photon.* **5** 682–7